One Health 16 (2023) 100554

Contents lists available at ScienceDirect

One Health

journal homepage: www.elsevier.com/locate/onehlt

Japanese encephalitis transmission trends in Gansu, China: A time series predictive model based on spatial dispersion

Xuxia Wang [a,1], Aiwei He [a,1], Chunfang Zhang [a], Yongsheng Wang [b], Jing An [a], Yu Zhang [a,c,*], Wenbiao Hu [d,**]

[a] Gansu Center for Disease Control and Prevention, Lanzhou, Gansu, China
[b] Evidence-Based Social Science Research Center/Health Technology Assessment Center, School of Public Health, Lanzhou University, Lanzhou, Gansu, China
[c] Chinese Center for Disease Control and Prevention, Changping, Beijing, China
[d] School of Public Health and Social Work, Queensland University of Technology, Brisbane, QLD, Australia.

ARTICLE INFO

Keywords:
Japanese encephalitis
Infectious diseases
Public health
Epidemiology

ABSTRACT

Objective: This study serves to ascertain trends of space and time for Japanese encephalitis (JE) transmission at the township-level and develop an innovative time series predictive model to predict the geographical spread of JE in Gansu Province, China.

Methods: We collected weekly data on JE from 2005 to 2019 at the township-level. Kriging interpolation maps were used to visualize the trend of the epidemic spread of JE, and linear regression models were used to calculate the monthly changes in minimum longitude and maximum latitude of emerging towns with JE to assess the speed of the epidemic's spread to the northwest. Additionally, we utilized a time series Seasonal Autoregressive Integrated Moving Average (SARIMA) model to dynamically predict the ongoing weekly number of JE emerging townships.

Results: The Kriging difference map revealed a significant trend of JE spread towards the northwest. Our regression model indicated that the rate of decrease in minimum longitude was approximately 0.64 km per month, while the rate of increase in maximum latitude was approximately 1.00 km per month. Furthermore, the SARIMA pattern $(2,0,0)(2,0,1)_{52}$ exhibited a better goodness-of-fit for predicting JE transmission, with an overall agreement of 93.27% to 94.23%.

Conclusion: Our study highlights the expansion of JE cases towards the northwest of Gansu, indicating the need for ongoing surveillance and control efforts. The use of the SARIMA model provides a valuable tool for predicting the trend of JE spatial dispersion, thereby improving early warning systems. Our findings suggest that the number of emerging townships can be used to predict the trend of JE spatial dispersion, providing crucial insights for future research on JE incidence.

1. Introduction

JE is a zoonotic illness transmitted by arthropods and caused by the Japanese encephalitis virus (JEV). It can result in death or serious disability [1,2]. JEV circulates among various hosts, with aquatic wading birds serving as reservoir hosts, pigs as amplification hosts, and humans and equids as terminal hosts. The main vector for JEV is the Culex mosquito species [3]. The occurrence of JE is closely tied to the natural environment and the distribution of the Culex mosquito vector. Children under the age of 15 are primarily affected by JE, with a fatality rate of 30–40% [4,5]. Additionally, 30–50% of survivors may experience severe neurological and mental sequelae [6,7]. Following the introduction of JE vaccines, the proportion and the absolute number of cases among adults increased [8].

JE is a significant neurological disease in Asia, causing an estimated 67,900 cases each year, with approximately 10,000 fatalities worldwide and 50% of cases occurring in China [9,10]. The NEPI (National Expanded Program on Immunization) has significantly reduced the

* Corresponding author at: Gansu Center for Disease Control and Prevention, Lanzhou, Gansu, China.
** Corresponding author at: School of Public Health and Socia Work, Queensland University of Technology, Brisbane, QLD, Australia
E-mail addresses: zhangyu@ninh.chinacdc.cn (Y. Zhang), w2.hu@qut.edu.au (W. Hu).
[1] These authors contributed equally to this work.

https://doi.org/10.1016/j.onehlt.2023.100554
Received 8 July 2022; Received in revised form 25 April 2023; Accepted 25 April 2023
Available online 27 April 2023

incidence rate of JE in China. However, in recent years, the incidence rate of JE in Gansu Province has dramatically increased, causing it to have the highest incidence rate of JE in China. 95% of cases are among adults over 15 years old who have not been vaccinated against JE. The largest JE outbreak occurred in Gansu in 2018 with over 500 cases. Accurately identifying the spatiotemporal transmission of JE is critical for government decision-making. In our previous study, we used aggregated on 10-year period at country level (1958–2017) to map the spatial patterns of historic JE transmission in Gansu Province [11]. However, two issues remain to be resolved. First, it is unclear if the spatial transmission pattern of JE at country level observed at high aggregated data (10-year period) has any changes at finer spatial and temporal scales (i.e weekly and township level). Second, it is uncelar if it is possible to develop an innovative time series predictive model to timely predict the spatial dispersion of JE. Thus, the research aims to develop an innovative time series predictive model based on spatial disersion to predict future geographical dispersen of JE, using weekly JE data at townships.

2. Materials and methods

2.1. Study site

Located in northwestern China, Gansu Province encompasses 86 counties and has a population of 26.47 million (Gansu yearbook 2020). We obtained the town-level geographic vector polygon map from Gansu through the China CDC (2012 Edition). There are 1383 townships within its jurisdiction, as shown in Fig. 1.

2.2. Data collection

To gather data for this study, weekly information on Japanese Encephalitis (JE) at the township level was collected from the China Information System for Disease Control and Prevention (CISDCP) between 2005 and 2019. Nine cases (0.59%) had unknown town-level addresses during this period and were therefore excluded from the study. The diagnosis of JE cases was based on diagnostic criteria WS-214-2001 (used from 2005 to 2008) and WS-214-2008 (used from 2009 to the present). Confirmed cases, including both clinically diagnosed cases and laboratory-confirmed cases, were included in the study from 2005 to 2019.

The population proportion of each township within the jurisdiction of each county was calculated using LandScan™ data. LandScan™ is modelled by the Oak Ridge National Laboratory (ORNL) using space information, picture analysis, and a multi-variable asymmetric pattern method of disaggregating census counts in administrative boundaries (ORNL, 2016) [12,13]. The county population in the "Gansu Statistical Yearbook" was multiplied by the township population proportion to determine the population of each township. The LandScan™ resolution is rough and has a resolution of 1 km.

District boundary changes for each township in 2005–2019, were obtained from the Bureau of Statistics and the Department of Civil Affairs of Gansu. Each township of each year in Gansu corresponds to the township in the town-level geographic vector polygon map after adjusting for geographical boundary changes. If the administrative division of one township was split or merged, then the study data of split or merged townships for specific years were allocated in proportion to the population or summed for specific years. The study data were categorized into three groups: 2005–2009, 2010–2014, and 2015–2019, based on changes in the epidemic from the relatively normal epidemic period (2005–2009), lower epidemic period (2010–2014), and outbreak period (2015–2019).

2.3. Descriptive analysis

We used the ggplot2 function in R3.6.1 software to visualize the weekly distribution profiles of JE cases number in the heatmap format.

2.4. Spatial patterns analysis

We mapped JE incidence at the township level using ArcGIS software version 10.2 (ESRI, America) to display its spatial distribution. We used administrative divisions to summarize the JE incidence, but the shape and scale of administrative divisions could affect the incidence rate and cause MAUPs. Therefore, we chose Common Kriging for modelling data that exhibit spatial trends [14,15]. This method is widely used to produce a continuous spatial surface of diseases and can alleviate MAUPs [16,17]. We converted the average incidence map of each township into

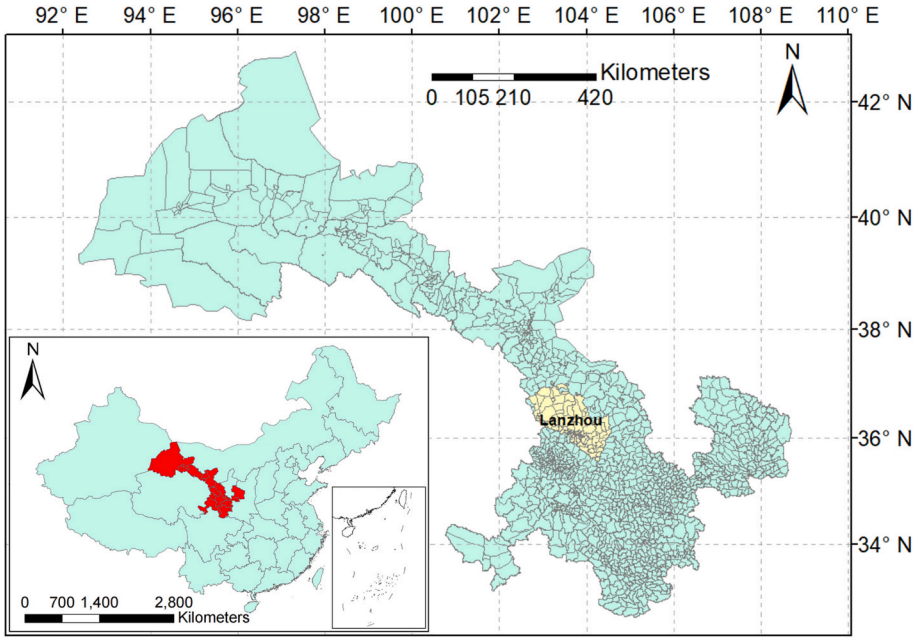

Fig. 1. Geographical administrative division at the township level, Gansu Province, China. These research domains as well as the position in Gansu and China. The picture was produced by means of ArcGIS software version 10.2 (ESRI, America).

an incidence map of the centroid of each township using ArcGIS 10.2 software and then created Kriging interpolation maps of JE incidence over three periods: 2005 to 2009, 2010 to 2014, and 2015 to 2019.

In addition, the spatial changes in epidemic areas are often as significant as the intensity of the epidemic, and this information can aid in the development of early warnings. To observe the changes in the prevalent areas of JE, we created maps of emerging townships with JE cases year by year. A township with the first case of JE during the study period is considered to be an emerging township of JE.

2.5. Dynamic spatial and temporal dispersion

The latitude and longitude of the centroid of each township were directly computed using ArcGIS 10.2 software. We used a linear regression model to investigate whether the JE endemic area expanded during 2005–2019 by observing changes in the min longitude and max latitude of emerging townships. A scatter plot with a regression line was used to illustrate the spread of JE at the min longitude and max latitude levels and estimate the speed of spread in the west and north. We performed all analyses using IBM SPSS Statistics software, version 25, and set statistical significance at $P < 0.05$. We thoroughly assessed the integrity and correctness of the data before conducting the analysis.

2.6. Time series seasonal decomposition

Temporal sequences were disintegrated into three parts: trend, seasonal, along with the remainder (residual). Season decomposition of time series by Loess decomposition information was shown in pictures by four panels: data (weekly JE emerging townships), trend (variance in data during the study), seasonal (variance in data during one year), together with the remainder (variance which remains behind deleting seasonal and trend parts) [18,19]. The season decomposition of temporal sequences with the Loess (STL) function using R 3.6.1 tidyverse package [20] during 2005–2019 was performed by us.

2.7. Time series SARIMA trend analysis

We utilized the Seasonal Auto-Regressive Integrated Moving Average (SARIMA) model to forecast outbreaks of infectious diseases [21,22]. This model is particularly suitable for analyzing infectious disease surveillance data with autocorrelation [23,24]. In general, six parameters are selected when fitting this model: (p, d, q) (P, D, Q), where p represents the order of autoregression (AR), d represents the order of integration, and q represents the order of moving average (MA) [25]. The seasonal part has three parameters denoted as P, D, and Q [26]. These parameters resemble p, d, and q but are conducted on the scale of periodicity (52 weeks). For instance, $P = 1$ indicates an autoregressive term of order 1 on the annual scale, i.e., the value in any week. The orders of AR and MA models are determined by analyzing the Autocorrelation Function (ACF) and Partial Autocorrelation Function (PACF). In this research, the goodness-of-fit of the model was evaluated by computing autocorrelation for residuals.

To enhance the forecast model, we used the weekly number of emerging townships with JE cases. To improve the fitting effects of the model, we first performed a square root conversion of the weekly number of emerging townships. Moreover, to examine the model's forecasting capacity, we divided the data into two datasets. Specifically, data from January 1, 2005, to December 31, 2017 (a total of 676 weeks) were used as the training set to establish a SARIMA model, and data from January 1, 2018, to December 31, 2019 (a total of 104 weeks) were used as the testing dataset to validate the model. Secondly, we used ongoing dynamic weekly predictions for 2018–2019 data. Finally, we defined an outbreak when the number of emerging townships exceeded 25%, 50%, and 75% of the median number of emerging townships in Gansu over the study period and accurately determined the sensitivity and specificity of the prediction. IBM SPSS Statistics software version 25 was used for all data analysis. Statistical significance was defined at $P < 0.05$, and the integrity and correctness of the data were assessed before analysis.

3. Results

3.1. JE epidemics and outbreaks

Between 2005 and 2019, the distribution range and annual incidence of JE in Gansu exhibited an initial decline followed by an increase. Fig. 2 shows that an outbreak of JE occurred in the province in 2018, with cases reported in 290 townships across 55 counties. The incidence rate in 2018 was 1.92/100,000, marking the highest value observed in the past 15 years. In contrast, 2012 saw the lowest incidence rate of 0.02/100,000, with only six townships in five counties reporting cases of JE.

3.2. Time pattern of JE cases

During the study period, the JE epidemic in Gansu Province typically occurred between weeks 14–30 and 35–51, with the highest incidence rates observed around week 33. A majority (93.35%) of cases were reported between weeks 29–37, as depicted in Fig. 3.

3.3. Dynamic spatial and temporal dispersion

The incidence rate of each township in Gansu Province was calculated in three stages, and Kriging interpolation maps of incidence were generated to analyze the trend of JE epidemic ranges. From 2005 to 2009, 97 townships with high incidence rates (≥2/100,000) were identified, all of which were distributed in the southeastern region. From 2010 to 2014, the number of townships with high incidence rates also decreased significantly to 39, still mainly distributed in the southeastern region. However, from 2015 to 2019, the number of townships with high incidence rates increased significantly to 243, showing a trend of expansion from the southeast to the northwest. (shown in Fig. 4).

3.4. JE emerging-township analysis

From 2005 to 2019, JE cases were reported in 529 out of the 1383 townships in Gansu Province, accounting for 38.25% of all townships. The cases were concentrated in the region between 32.70°N, 100.45°E and 38.70°N, 108.54°E. Emerging epidemic areas were observed each year from 2005 to 2019, with new townships mainly distributed in the southeastern region of Gansu Province from 2006 to 2009, with 93, 26, 22, and 21 townships each year, respectively. The number of new townships in this region decreased from 2010 to 2014, with 11, 6, 2, 14, and 4 townships reported each year, respectively. However, in the past five years (2015–2019), there has been a trend of spreading from the southeast to the northwest, with 2, 34, 139, 106, and 11 new townships reported each year. Cases have also been reported in the previously non-infected Hexi Corridor, with an epidemic occurring in Ganzhou District of Zhangye Municipality in 2009. In 2017, epidemics occurred in Minqin County, Gulang County, and Tianzhu County of Wuwei Municipality, and in 2018, epidemics occurred in Jinchuan District and Yongchang County of Jinchang Municipality. In addition, an epidemic occurred in Liangzhou District of Wuwei Municipality in 2019. (SeeFig. 5 for a visual representation of the data).

According to Supplementary Fig. 1, the min longitude of JE emerging townships displayed a decreasing trend of 0.007 per month ($P = 0.034$), while the max latitude of JE emerging townships exhibited an increasing trend of 0.009 per month ($P = 0.012$). To evaluate the distance between the changes in min longitude and max latitude, we made a rough calculation, which suggests that the min longitude decreases at a rate of 0.64 km per month, whereas the max latitude increases at a rate of 1.00 km per month.

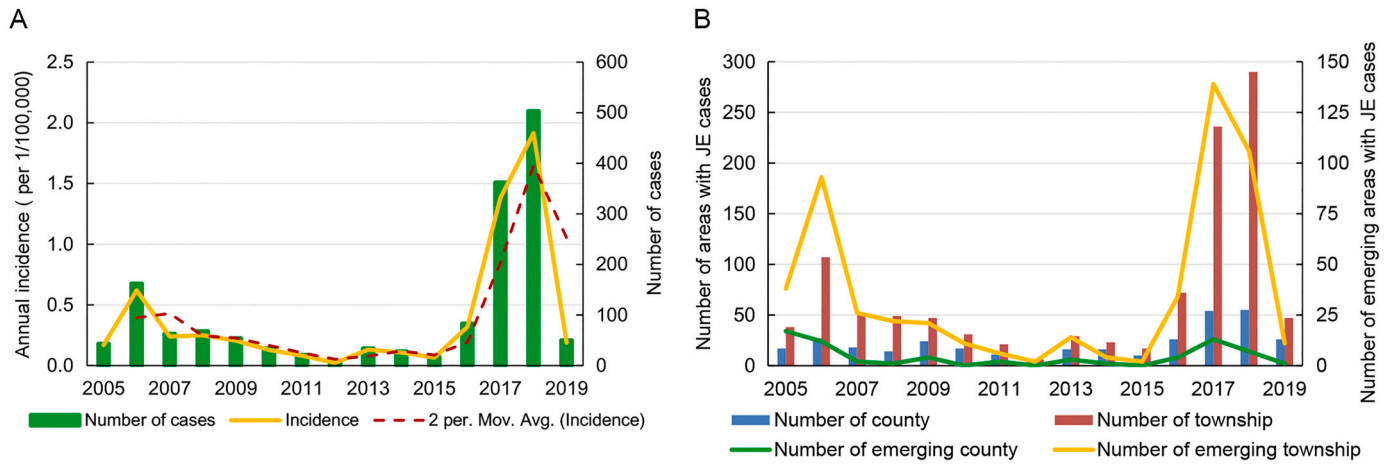

Fig. 2. JE incidence in Gansu Province, 2005–2019. A: Annual incidence as well as moving average of JE incidence from Gansu Province, 2005–2019. B: The number of counties as well as townships with JE cases of Gansu Province, 2005–2019.

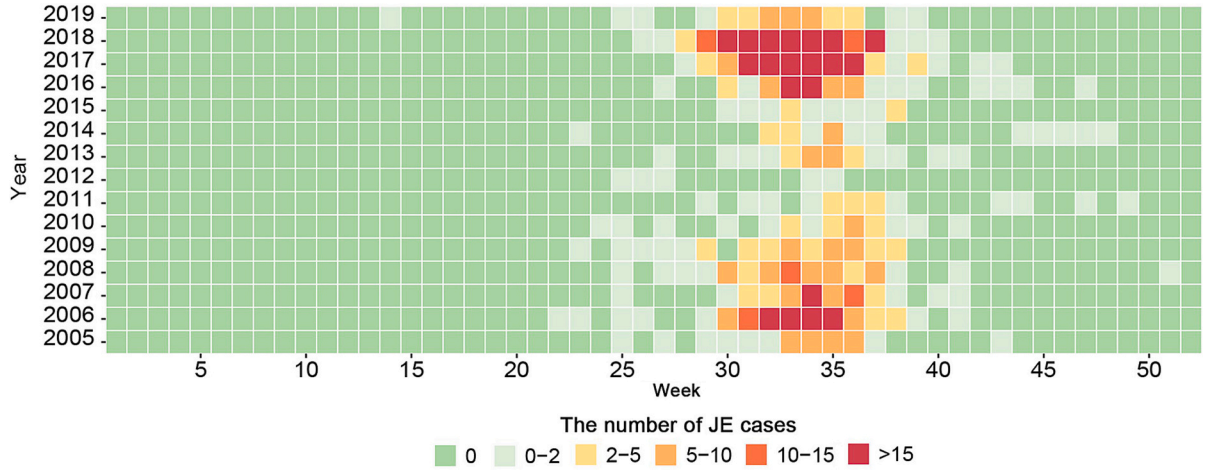

Fig. 3. Heatmap representing the weekly number of JE cases of each year in Gansu Province. The horizontal dimension indicates the weekly JE infection, while the ordinate represents the year. The color of the cells represents the magnitude of the number of JE cases in that cell.

3.5. Time series seasonal decomposition

The weekly number of JE emerging townships, trend, seasonal and residual (remainder) parts were analyzed using STL decomposition, as shown in Supplementary Fig. 2. The results indicated that seasonality was the most prominent factor throughout the study period. Notably, the peak number of emerging towns was observed in 2017, which was earlier than the peak incidence rate observed in 2018.

3.6. Time series trend analysis

Supplementary Fig. 3 demonstrates that the SARIMA model $(2,0,0)(2,0,1)_{52}$ had a better goodness of fit for predicting JE transmission, with a statistical R^2 value of 74.5%. The parameter assessments and trial consequences for this pattern are presented in Supplementary table. The forecast curves corresponded well with the actual values, as seen in Fig. 6. When defining an outbreak as 25% above the median or 50% above the median, validation analyses revealed an overall agreement of predicted outbreaks at 93.27% (sensitivity: 7/10 = 70.00%, specificity: 90/94 = 95.74%, and crude agreement, (7 + 90)/104 = 93.27%), as shown in Table. 1. When stating an outbreak to be 75% above the median, validation analyses indicated an overall agreement of predicted outbreaks at 94.23% (sensitivity: 7/9 = 77.78%, specificity: 91/95 = 95.79%, and crude agreement, (7 + 91)/104 = 94.23%).

4. Discussion

In recent years, there has been a growing concern over the JE epidemic in Gansu, a province in northwest China [27]. Wu Dan et al. found that the recent outbreak of JE in Gansu was due to the onset of the disease in unvaccinated adults, with a different time and space distribution than that observed in children in the past [8]. Our study aimed to document the spatiotemporal distribution and spreading trend of JE in Gansu Province over the past 15 years, since the implementation of an internet-based JE reporting system in 2004 and the incorporation of the JE vaccine into the EPI in 2008. Our results indicate that the incidence of JE in Gansu first declined, but then increased after more than ten years of vaccination. Spatial analysis at the township level revealed that the pandemic range of JE has enlarged, with more towns in the northwest becoming new epidemic areas, while cases remain clustered in the southeast. This emerging epidemic presents a new challenge for the prevention and control of JE.

The use of administrative divisions as geographic units to report incidence data may overestimate differences in incidence levels in border areas and lead to MAUPs. To alleviate this issue, we utilized Kriging interpolation techniques to better show the trend of disease distribution, while recognizing that such techniques may have a smoothing effect and under-appreciate high local worth or overrate low local worth. We produced a Kriging interpolation map based on

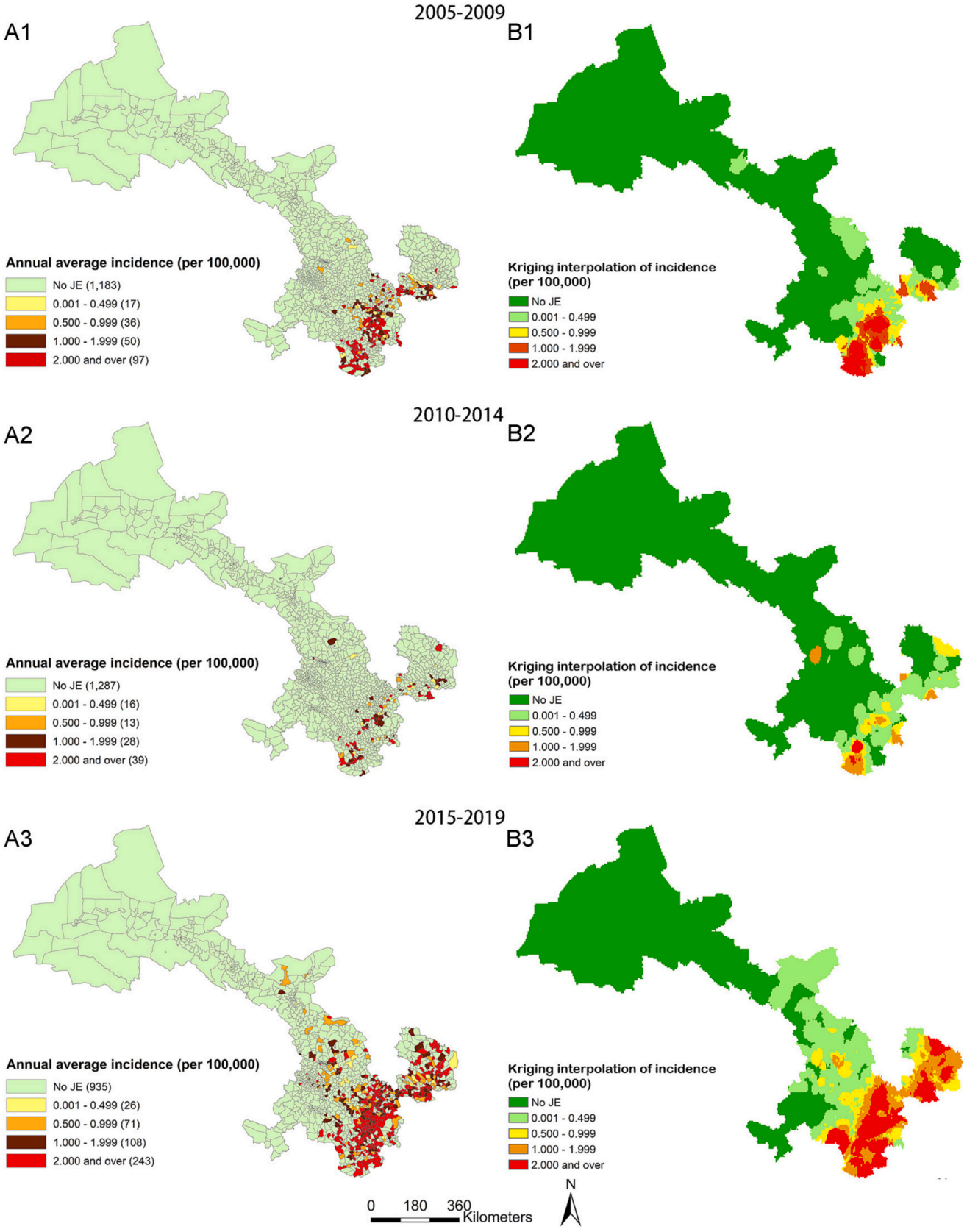

Fig. 4. Maps of JE annual incidence and Kriging interpolation of incidence in town-standard in Gansu Province. A: Maps of JE annual incidence at the township in Gansu Province for the periods of 2005–2009 (Fig. A1), 2010–2014 (Fig. A2), and 2015–2019 (Fig. A3); B: Kriging interpolation maps of JE incidence at the township in Gansu Province for the periods of 2005–2009 (Fig. B1), 2010–2014 (Fig. B2), and 2015–2019 (Fig. B3). This picture was produced by means of ArcGIS software version 10.2 (ESRI, America).

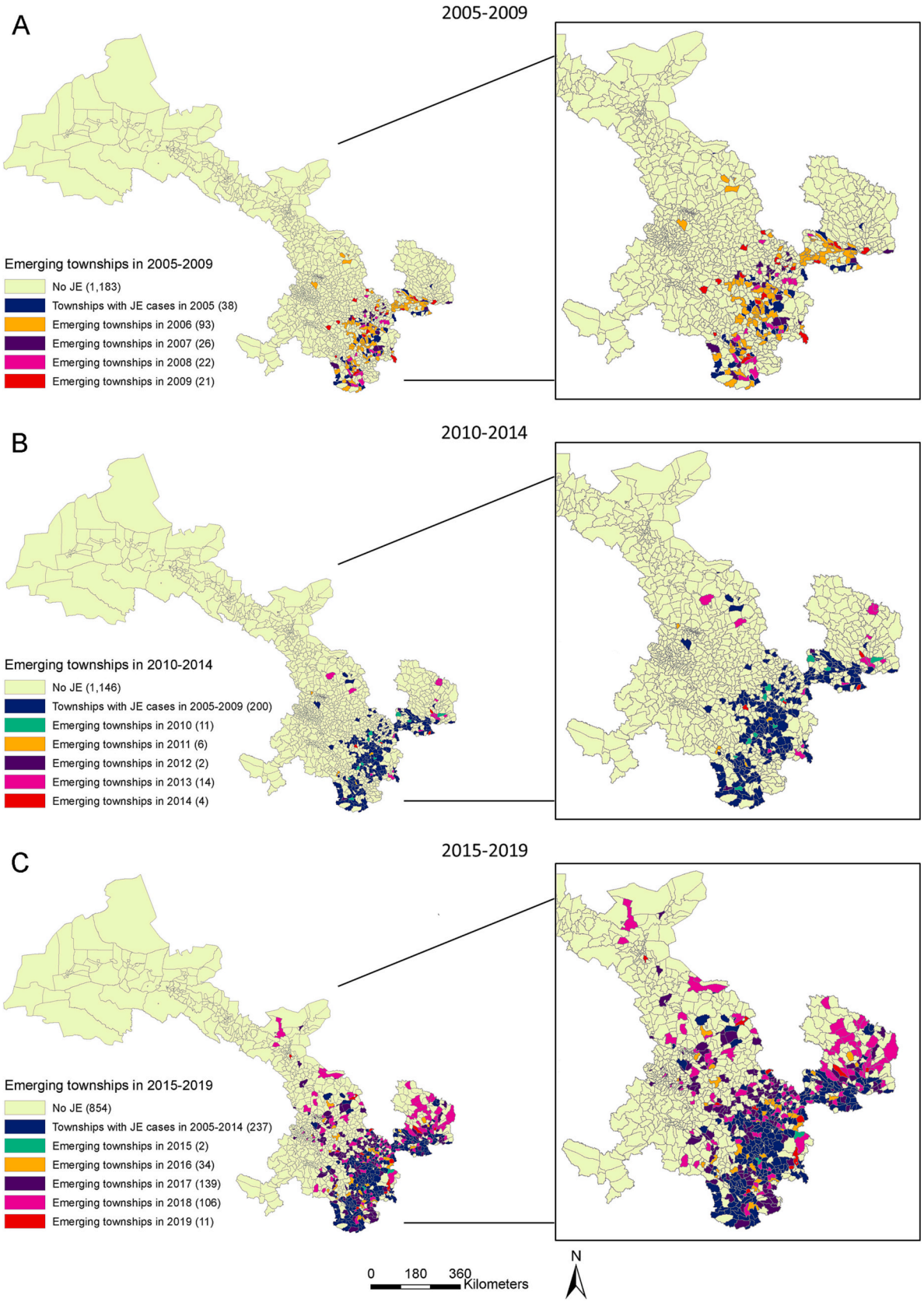

Fig. 5. Emerging townships maps of JE epidemic in Gansu Province. Emerging townships map of JE epidemic in Gansu Province for the periods of 2005–2009 (Fig. 5A), 2010–2014 (Fig. 5B) and 2015–2019 (Fig. 5C). The data was produced by means of ArcGIS software version 10.2 (ESRI, America).

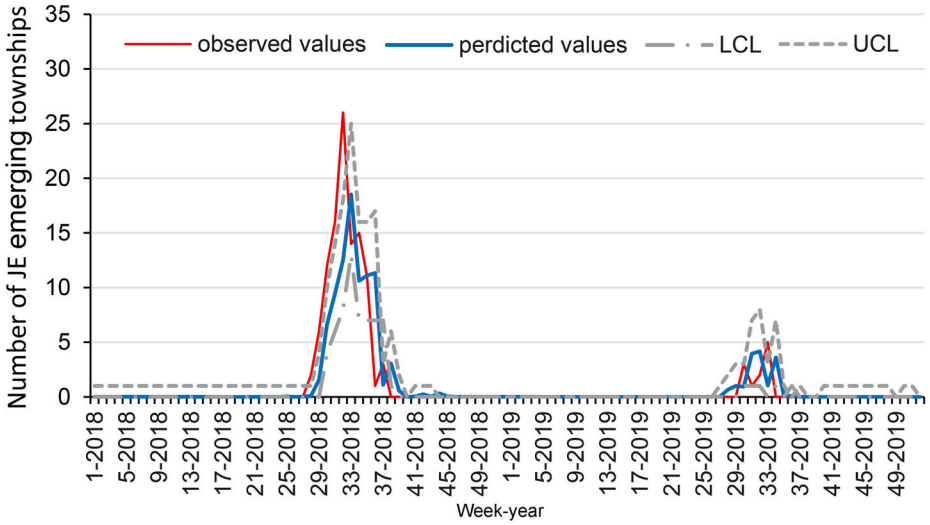

Fig. 6. Reported and Predicted the number of JE emerging townships by Week, 2018–2019.

Table 1
Sensitivity and specificity of SARIMA models for the number of JE emerging townships.

Actual	Predicted		Total
	Occurrence	Non-occurrence	
Define an outbreak as 25% above Median			
Occurrence	7	3	10
Non Occurrence	4	90	94
Total	11	93	104
Define an outbreak as 50% above Median			
Occurrence	7	3	10
Non Occurrence	4	90	94
Total	11	93	104
Define an outbreak as 75% above Median			
Occurrence	7	2	9
Non Occurrence	4	91	95
Total	11	93	104

incidence rates at the township level to observe changes in JE incidence trends during three stages of the study period.

Our previous research identified an extension of the JE pandemic, but did not provide a detailed description of its gradual extension over the past 15 years [11]. By analyzing data at the township level over the last 15 years, we found the range and intensity of JE has continued to expand in last five years, especially during outbreak years (2017–2018), with a clear trend of spreading to the northwest. From 2005 to 2009, the incidence of JE in Gansu Province was at a low to medium level nationwide. During this period, Gansu Province had not yet fully vaccinated eligible children with the JE vaccine. From 2010 to 2014, Gansu Province began universal vaccination of eligible children with the JE vaccine, resulting in a significant decrease in the number of emerging townships, and an incidence. However, the low prevalence led to a low positive rate of serum in the population. From 2015 to 2019, the JE incidence rebounded and the area of incidence expanded, with a historical peak in 2017–2018. To combat the disease, Gansu Province began vaccinating adults in key areas from 2018 to 2019 and implemented standardized prevention and control measures. As a result, the JE incidence dropped to 0.19/100,000 in 2019, with only 11 emerging townships.

We analyzed the geographical change trend of the distribution of emerging townships using latitude and longitude as observation indicators. Our study revealed that under the current epidemic trend, the epidemic range of JE in Gansu Province is spreading westward at a rate of 0.64 km per month and northwards at a rate of 1 km per month. This finding is consistent with the result of our Kriging interpolation map analysis, further confirming that the JE epidemic in Gansu Province has been expanding to the northwest in recent years. This also reminds us that without proper prevention and control measures, the epidemic may continue to spread to the west and north. Additionally, areas that were not previously affected by the epidemic should also be prepared to prevent and control new outbreaks.

Furthermore, the STL decomposition showed that the changing trend in the number of emerging townships with JE transmission was slightly different from that of the incidence rate, and the peak of the emerging township numbers occurred earlier than that of incidence. This suggests that when studying infectious diseases with low disease intensity but more serious disease burden and impact, the number of new regions may be more sensitive than other indicators such as the number of cases or the incidence rate.

Infectious disease prediction and early warning systems are crucial for effective decision-making and reducing mortality and morbidity. Early warning and prediction systems have been established worldwide to tackle infectious diseases [25,28–31]. However, the complexity of various influencing factors in reality often makes it difficult to use multiple regression models to quickly analyze and predict. The accurate simulation of models requires high requirements for parameter selection. In contrast, SARIMA models can fully considered the autocorrealtion, trend and seasonality issue in modelling, making short-term forecasting easy to implement and highly accurate [32,33]. However, the accuracy of recent historical data can have a significant impact on model extrapolation [34]. To improve prediction accuracy, our study used ongoing dynamic strategies by employing different SARIMA models at every time step (week) and utilizing the actual data at the previous step as input. This approach continuously updated the models, improving the prediction effect when rapidly predicting the trend of epidemic change. Our results showed that the overall agreement of predicted outbreaks was 93.27%–94.23%, which can inform health policy-makers for possible intervention (e.g. increasing insecticidal spraying, vaccination and community health education during high-risk period, improving the disease surveillance system etc.)

The significance of our study's results lies in the ability to quickly predict spatial dispersion trend and take targeted preventive and control measures based on more convenient data, or determine whether the actual incidence level fluctuates within the normal range based on predicted results. Our SARIMA models fit well, and the sensitivity and specificity of detecting abnormal diffusion are high, enabling the quick detection of JE trends. However, any SARIMA prediction model has its limitations, and the predicted results of our model are mainly intended

to judge whether the actual incidence trend fluctuates within the normal range, alert the outbreak or epidemic of the epidemic, and are not suitable for predicting the specific value of the incidence. Therefore, the results should be interpreted with care when used.

Our study has several strengths, including China's well-functioning, centrally managed, internet-based JE reporting system that involves case-by-case management. This allows us to use detailed residential addresses in the system to analyze the distribution characteristics of JE on a town level. Our study is also the first to use emerging townships in a time series forecast study of JE in Gansu Province, providing technical support for the development of early warning and forecasting systems. This information is valuable to decision-makers in developing suitable prevention measures. However, since JE is vulnerable to climate, our study's limitations include not exploring possible menace elements associated with clustering. Thus, our next study will focus on JE transmission and related environmental factors, including climatic, ecological, and sociodemographic factors in Gansu, and build more sophisticated and complex forecasting models.

5. Conclusion

Our study's findings offer more specific evidence for local JE control's public health implications, especially in identifying high-risk areas at the township level. Moreover, the study illustrates the practicality of using the number of emerging townships to detect JE epidemics in real-time. This could be seen as a prerequisite for building early warning systems that take socio-environmental changes into account.

Ethical approval

This research was allowed by the Ethics Committee of Gansu Provincial Centers for Disease Control and Prevention (No: 2020011 as well as the date of approval: 10 April 2020).

Author statement

Xuxia Wang: Conceptualization, Methodolog, Formal analysis, data curation, writing – original draft, visualization.

Yu Zhang, Chunfang Zhang, Yongsheng and Jing An: review and editing.

Wenbiao Hu: Conceptualization, Methodology, review and editing.

Declaration of Competing Interest

All authors claim that they don't have any collision of benefit.

Data availability

The authors do not have permission to share data.

Acknowledgment

This work was supported by the National Natural Science Foundation of China (grant number 82060614). We would like to express our gratitude to the Rural Division of Gansu Provincial Statistics Bureau for providing us with research background data and information.

Appendix A. Supplementary data

Supplementary data to this article can be found online at https://doi.org/10.1016/j.onehlt.2023.100554.

References

[1] D. Ghosh, A. Basu, Japanese encephalitis-a pathological and clinical perspective, PLoS Negl. Trop. Dis. 3 (9) (2009), e437.
[2] L. Turtle, T. Solomon, Japanese encephalitis - the prospects for new treatments, Nat. Rev. Neurol. 14 (5) (2018) 298–313.
[3] S.I. Yun, Y.M. Lee, Japanese encephalitis: the virus and vaccines, Hum. Vaccin. Immunother. 10 (2) (2014) 263–279.
[4] L.H. Wang, et al., Japanese encephalitis outbreak, Yuncheng, China, 2006, Emerg. Infect. Dis. 13 (7) (2007) 1123–1125.
[5] Y. Zheng, et al., Japanese encephalitis and Japanese encephalitis virus in mainland China, Rev. Med. Virol. 22 (5) (2012) 301–322.
[6] D. Ding, et al., Long-term disability from acute childhood Japanese encephalitis in Shanghai, China, Am. J. Trop. Med. Hyg. 77 (3) (2007) 528–533.
[7] L.J. Basumatary, et al., Clinical and radiological spectrum of Japanese encephalitis, J. Neurol. Sci. 325 (1–2) (2013) 15–21.
[8] D. Wu, et al., Emergence of Japanese encephalitis among adults 40 years of age or older in northern China: Epidemiological and clinical characteristics, Transbound. Emerg.Dis. 68 (6) (2021) 3415–3423.
[9] G.L. Campbell, et al., Estimated global incidence of Japanese encephalitis: a systematic review, Bull. World Health Organ. 89 (10) (2011) 766–774, 774A-774E.
[10] J.P. Caldwell, L.H. Chen, D.H. Hamer, Evolving epidemiology of Japanese encephalitis: implications for vaccination, Curr. Infect. Dis. Rep. 20 (9) (2018) 30.
[11] X. Wang, et al., Long-term epidemiological dynamics of Japanese encephalitis infection in Gansu Province, China: a spatial and temporal analysis, Am. J. Trop. Med. Hyg. 103 (5) (2020) 2065–2076.
[12] E.J. Flies, et al., Improving public health intervention for mosquito-borne disease: the value of geovisualization using source of infection and LandScan data, Epidemiol. Infect. 144 (14) (2016) 3108–3119.
[13] A.J. Tatem, et al., The effects of spatial population dataset choice on estimates of population at risk of disease, Popul. Health Metrics 9 (2011) 4.
[14] S. Tadesse, F. Enqueselassie, S.H. Gebreyesus, Estimating the spatial risk of tuberculosis distribution in Gurage zone, southern Ethiopia: a geostatistical kriging approach, BMC Public Health 18 (1) (2018) 783.
[15] R.S. Kirby, E. Delmelle, J.M. Eberth, Advances in spatial epidemiology and geographic information systems, Ann. Epidemiol. 27 (1) (2017) 1–9.
[16] N. Wang, et al., Lung Cancer mortality in China: spatial and temporal trends among subpopulations, Chest 156 (5) (2019) 972–983.
[17] M. Tuson, et al., Overcoming inefficiencies arising due to the impact of the modifiable areal unit problem on single-aggregation disease maps, Int. J. Health Geogr. 19 (1) (2020) 40.
[18] T. Silawan, et al., Temporal patterns and forecast of dengue infection in Northeastern Thailand, Southeast Asian J. Trop. Med. Public Health 39 (1) (2008) 90–98.
[19] F. Cortes, et al., Time series analysis of dengue surveillance data in two Brazilian cities, Acta Trop. 182 (2018) 190–197.
[20] R.P. Hafen, et al., Syndromic surveillance: STL for modeling, visualizing, and monitoring disease counts, BMC Med. Inform. Decis. Mak. 9 (2009) 21.
[21] U. Helfenstein, Box-Jenkins modelling in medical research, Stat. Methods Med. Res. 5 (1) (1996) 3–22.
[22] U. Helfenstein, The use of transfer function models, intervention analysis and related time series methods in epidemiology, Int. J. Epidemiol. 20 (3) (1991) 808–815.
[23] R.P. Soebiyanto, F. Adimi, R.K. Kiang, Modeling and predicting seasonal influenza transmission in warm regions using climatological parameters, PLoS One 5 (3) (2010), e9450.
[24] W. Hu, et al., Dengue fever and El Nino/Southern Oscillation in Queensland, Australia: a time series predictive model, Occup. Environ. Med. 67 (5) (2010) 307–311.
[25] Y. Zhang, et al., Monitoring pertussis infections using internet search queries, Sci. Rep. 7 (1) (2017) 10437.
[26] R.J. Hyndman, Y. Khandakar, Automatic time series forecasting: the forecast package for R, J. Stat. Softw. 27 (3) (2008) 1–22.
[27] X. Li, et al., An outbreak of Japanese encephalitis in adults in northern China, 2013: a population-based study, Vector Borne Zoonotic Dis. 19 (1) (2019) 26–34.
[28] J.C. Semenza, Prototype early warning systems for vector-borne diseases in Europe, Int. J. Environ. Res. Public Health 12 (6) (2015) 6333–6351.
[29] L.F. Chaves, M. Pascual, Comparing models for early warning systems of neglected tropical diseases, PLoS Negl. Trop. Dis. 1 (1) (2007), e33.
[30] P.B. Miller, et al., Forecasting infectious disease emergence subject to seasonal forcing, Theor. Biol. Med. Model. 14 (1) (2017) 17.
[31] W. Yang, et al., A nationwide web-based automated system for outbreak early detection and rapid response in China, Western Pac. Surveill. Response J. 2 (1) (2011) 10–15.
[32] F. Liu, et al., Application of R-based multiple seasonal ARIMA model, in predicting the incidence of hand, foot and mouth disease in Shaanxi province, Zhonghua Liu Xing Bing Xue Za Zhi 37 (8) (2016) 1117–1120.
[33] Y. Peng, et al., Application of seasonal auto-regressive integrated moving average model in forecasting the incidence of hand-foot-mouth disease in Wuhan, China, J. Huazhong Univ. Sci. Technol. Med. Sci. 37 (6) (2017) 842–848.
[34] M.M. Kuan, Applying SARIMA, ETS, and hybrid models for prediction of tuberculosis incidence rate in Taiwan, PeerJ 10 (2022), e13117.

Wang Xu Xia, female, born in 1976, Master, majoring in Environmental Epidemiology and Infectious Diseases.

He Ai Wei, male, born in 1979, Undergraduate, majoring in Infectious Diseases.